Chapter 3
Nuclear Architecture, Chromosome Aberrations, and Genetic Damage

Gustavo A. Folle, María Vittoria Di Tomaso, Laura Lafon-Hughes, and Pablo Liddle

Abstract Mammalian interphase nuclei are highly organized structures in which chromosome territories are nonrandomly distributed following a radial pattern. Gene richness and size markedly influence nuclear chromosome positioning. Active euchromatin and inactive heterochromatin exhibit different nuclear topology: the former is centrally located and the latter mostly placed at the periphery, within chromocenters, and around nucleoli. DNA is subjected to a wide repertoire of insults including radiation, chemical, and biological agents. The differential sensitivity of euchromatin and heterochromatin to clastogens has been a matter of debate, although most experimental evidence supports that euchromatin is more damage prone. Gene expression and DNA synthesis coupled to chromatin remodeling could act as key factors in the distribution of chromosome aberrations (CA) in euchromatic and heterochromatic regions of genome. In this chapter, the main features of nuclear architecture as well as an overview of current knowledge of genetic damage at the metaphase and interphase levels are presented. Also, the preferential involvement of transcriptionally active regions of the human genome regarding the induction of chromosome aberrations and deregulation of tumor genes is analyzed. Finally, the impact of DNA replication timing and connected chromatin remodeling processes in the generation and localization of CA and primary genetic damage is discussed.

G.A. Folle (✉) • M.V. Di Tomaso • L. Lafon-Hughes • P. Liddle
Department of Genetics, Instituto de Investigaciones Biológicas, Clemente Estable (IIBCE), Av. Italia 3318 CP, 11600 Montevideo, Uruguay
e-mail: folle@iibce.edu.uy; marvi@iibce.edu.uy; laulaf@iibce.edu.uy; liddle@iibce.edu.uy

Y.B. Yurov et al. (eds.), *Human Interphase Chromosomes: Biomedical Aspects*,
DOI 10.1007/978-1-4614-6558-4_3, © Springer Science+Business Media, LLC 2013

Introduction

Human populations exhibit a significant frequency of inborn chromosomal aberrations (CA). Therefore, it is of utmost importance to understand the mechanisms underlying their origin and transmission to progenies (Miller and Therman 2001). CA are among the major biological endpoints of human exposure to ionizing radiation and genotoxic compounds. Hence, CA scoring is a key tool for biological dosimetry of radiation exposure or disclosing putative mutagenic/carcinogenic agents. Moreover, specific CA are associated with different types of cancers (Obe et al. 2002).

Early cytogenetic analyses based on classical solid staining of metaphase chromosomes provided valuable information on the types and frequencies of spontaneous and clastogen-induced CA. Exposure of cells during the G_0/G_1-phase leads to chromosome-type aberrations whereas chromatid-type lesions are induced after DNA replication (S/G_2 phases). Chromosome banding procedures allowed the precise recognition of individual chromosomes, karyotype evolutionary studies, and assignment of genes to specific chromosome landmarks as well as accurate mapping of chromosome breakpoints either induced by DNA-damaging agents or present in inborn or neoplastic diseases.

Moreover, banding techniques paved the way to understanding the highly complex structure of mammalian chromosomes. G- and R-banding revealed the presence of alternate Giemsa-dark and Giemsa-light chromosome bands, which reflect the evolutionary partition of euchromatin as well as constitutive and facultative heterochromatin into distinct chromosome domains. G-light bands are gene-rich, high G-C content, early-replicating regions, harboring short interspersed repeated elements (SINEs). Most housekeeping genes map to G-light bands and exhibit distinct epigenetic modifications such as unmethylated CpG islands and histone H3/H4 hyperacetylation. On the other hand, G-dark bands are gene-poor, late-replicating, A-T-rich regions, homing tissue-specific genes and long interspersed repeated elements (LINEs). C-band constitutive heterochromatin is highly packed, inactive, and almost devoid of genes. Epigenetic modifications in G-dark and C-bands include DNA and specific histone lysine methylation as well as serine H3/H4 underacetylation (Holmquist 1992; Korenberg and Rykowski 1988).

The impact of chromatin organization in the induction and localization of genetic damage induced by clastogens has been extensively studied by several research groups (Obe et al. 2002 and citations therein). The interchromosomal distribution of CA seems to be random (Cornforth et al. 2002; Martínez-López et al. 2000), although nonrandomness has also been claimed (Grigorova et al. 1998; Xiao and Natarajan 1999) analyzing either G-banded or FISH-painted chromosomes. In contrast, the intrachromosomal distribution of CA has been repeatedly reported to be nonrandom (Obe et al. 2002; Slijepcevic and Natarajan 1994). A higher susceptibility of G-light chromatin in Chinese hamster ovary (CHO) cells after electroporation of restriction endonucleases (RE) or DNAse I or even following irradiation with neutrons and γ-rays has been reported. Moreover, clustering of both endonuclease- and radiation-induced breakpoints in specific CHO chromosome regions independently of the cell-cycle stage (G_1- or S-phase) was also evidenced (Folle and Obe 1995, 1996; Folle et al. 1997, 1998).

Immunolabeling of hyperacetylated histone H4 ($H4^{+a}$) in CHO metaphase spreads revealed the colocalization of $H4^{+a}$ chromosome regions with endonuclease- and radiation-induced breakpoint clusters, giving further support to the assumption that transcriptionally active euchromatin is a preferential target for DNA damage induction (Martínez-López et al. 2001).

The detection of specific DNA sequences and even whole chromosomes (or chromosome arms) in metaphase spreads through fluorescence in situ hybridization (FISH) techniques has greatly improved our knowledge regarding the mechanisms involved in the formation of CA. FISH analyses uncovered CA types and mechanisms not evidenced by conventional staining or banding procedures (Simpson and Savage 1995). Molecular cytogenetic techniques such as spectral karyotyping (SKY), comparative genome hybridization (CGH), multicolor FISH (mFISH), and multicolor chromosome banding (mBAND FISH) precisely identify a wide spectrum of CA ranging from drastic genomic alterations to minute chromosome changes. Interphase cytogenetic studies based on FISH or immunoFISH methods have furnished crucial information concerning the organization and function of eukaryotic chromosomes and nuclei. Correlative metaphase and interphase cytogenetic studies are now possible, especially in relationship to the origin and fate of CA. Still, our present understanding of DNA damage processing leading to CA formation remains incomplete.

Nuclear Architecture

The eukaryotic nucleus is a highly organized and compartmentalized structure reflecting genome and epigenome dynamics at the cellular and molecular level. The first compaction level of chromatin is the 10-nm fiber involving DNA wrapped around nucleosomes. Further chromatin folding could lead to the 30-nm fiber and to still poorly known higher-order structures critical for the building and dynamics of eukaryotic nuclei. Chromatin compaction levels seem to play a critical role in nuclear organization. Highly packed constitutive and facultative heterochromatin (C- and G-dark bands) reside at the nuclear periphery, around nucleoli, and within chromocenters whereas euchromatin (G-light bands) is centrally located (Postberg et al. 2010). The position of interphase chromosomes inside mammalian nuclei is nonrandom and radially organized. Chromosome positioning is mainly modulated by size and gene density but not by gene expression (Küpper et al. 2007). However, chromosome nuclear location may vary depending on cell type and shape, differentiation state, presence of chromosomal aberrations, senescence, and transformation. Interphase chromosomes are structured as discrete, nonoverlapping territories (CTs), although intermingling of peripheral chromatin loops was also proposed (Branco and Pombo 2006). Gene-rich chromosomes are inwardly positioned and gene-poor chromosomes mostly lodge in the nuclear boundary (Cremer et al. 2003). This chromosome gene richness-dependent topological partition has been shown to be evolutionarily conserved (Tanabe et al. 2002).

It is noteworthy that plasticity seems to be also an inherent feature of nuclear architecture, as evidenced by striking nuclear multilobation in granulocytes, and manifold modifications in cancer cells, as well as the striking relocation of euchromatin and heterochromatin in retina rod cells to improve light collection in nocturnal species (Solovei et al. 2009).

A central role of nuclear chromatin assembly could be the configuration of two distinct functional domains: condensed silent heterochromatin and transcriptionally active euchromatin. Packed heterochromatin shows low acetylating levels as well as methylated DNA and H3K9/H3K27 histone tail methylation whereas open euchromatin is highly acetylated and enriched in H3K4me and H3K79me. Nuclear chromatin compartments also influence gene expression and DNA synthesis patterns. In fact, transcription dominates in central regions although it is nearly absent from the nuclear rim (Sadoni et al. 1999, 2004). Furthermore, transcriptional hubs could be very significant for high throughput transcription and the expression of coregulated genes. DNA synthesis progression from early-replicating gene-rich to mid-/late-replicating gene-poor chromatin compartments is also highly ordered (see following).

According to the CT/IC model, CTs are bordered by the interchromatin compartment (IC), which harbors nuclear bodies and the complex machineries required for DNA transcription, replication, and repair as well as for RNA processing. The IC comprise an intricate channel network that expands throughout the nucleus, reaching the interior of CTs and the nuclear pores. The interface between CTs and the IC, named the perichromatin region (PR), has been proposed as a key nuclear subcompartment for DNA/RNA metabolism (Postberg et al. 2010; Rouquette et al. 2009).

DNA Damage and Chromosome Aberrations: The Nuclear Landscape

The DNA double-strand break (DSB) is the ultimate lesion leading to chromosomal aberrations, genomic instability, oncogenic transformation, and cell death (Obe et al. 2002). DSB may arise as a result of endogenous oxidative damage by oxygen free radicals or collapsed replication forks during DNA synthesis. A wide spectrum of physical, chemical, and biological DNA-damaging agents are also able to induce DSB. Two main repair systems evolved to cope with these deleterious and highly recombinogenic DNA lesions: nonhomologous end-joining (NHEJ), mostly active during the G_1 stage of the cell cycle, and homologous recombination (HR), which acts along late S/G_2-phases and requires an undamaged template for efficient DSB repair (Rogakou et al. 1998). DSB mobility is constrained within the nuclear volume and normally is not beyond 0.5 μm, which corresponds to the Brownian motion radius in cells (Jakob et al. 2009).

DNA damage triggers a global response in cells named DNA damage response (DDR), which activates a complex mechanism committed to detect lesions and restore DNA integrity. The induction of DSB elicits the phosphorylation of the variant histone H2AX on serine 139 (γH2AX) by PIKK (phosphoinositide 3-kinase-related kinase) ATM. Other PIKKs such as ATR and DNA-PKcs may also phosphorylate histone H2AX. Soon after DSB induction (~3 min), γH2AX molecules are generated over megabase chromatin domains flanking the lesion. A plateau in the yield of γH2AX foci is reached approximately 30 min after damage induction. In addition to signaling the presence of DSB, γH2AX molecules interact and may provide docking sites for repair proteins including the MRE11/NSB1/RAD50 complex, MCD1, 53BP1, and BRCA1. The H2AX phosphorylation response can be unveiled as discrete foci through immunodetection with specific antibodies allowing the quantitation of primary DNA lesions in interphase nuclei. As H2AX phosphorylation is proportional to DSB induction, γH2AX is considered a sensitive biomarker of DNA damage (Podhorecka et al. 2010). However, the presence of spontaneous γH2AX foci in human confluent fibroblast cultures and senescent cells as well as in aged mice tissues has been reported. S-phase cells exhibit distinct punctuate small γH2AX foci (Costes et al. 2010 and citations therein).

The distribution of γH2AX foci in the different nuclear compartments after DNA insult has been extensively studied. A preferential localization of γH2AX foci in the nuclear interior after treating human fibrosarcoma H1080 cells with UV radiation or hydrogen peroxide was observed. XRCC repair proteins also mapped to the same nuclear domains (Gazave et al. 2005). Modulation of γH2AX foci distribution by chromatin density was also reported by Costes et al. (2010). In this study, foci located mainly in DAPI-weak regions (euchromatin) or at eu- and heterochromatin interfaces. Moreover, exclusion of γH2AX foci from heterochromatin was also observed in MCF7 breast carcinoma cells treated with either X-rays or the topoisomerase II inhibitor etoposide. Combined immunodetection of HP1 (heterochromatin protein 1) evidenced no colocalization with γH2AX foci. Comparable results were obtained when the heterochromatin marker H3K9me3 was assayed. Interestingly, γH2AX foci mapped to heterochromatin domains and colocalized with HP1 when MCF7 cells were treated with hydroxyurea during late S-phase (heterochromatin replication). In this case, DSB stem from stalled or collapsed replication forks and ATR signaling. It is envisaged that chromatin remodeling associated to DNA synthesis could render heterochromatin amenable to histone H2AX phosphorylation (Cowell et al. 2007). Finally, it has been shown that specific heterochromatic regions such as the alpha satellite and satellite 2 are resistant to the formation of γH2AX foci after irradiation. Still, pretreatment of cells with the deacetylase inhibitor trychostatin A (TSA) causes these satellite sequences to be prone to generate γH2AX foci (Karagiannis et al. 2007).

These findings argue in favor of a higher sensitivity of euchromatin to DNA insult. On the other hand, they challenge the hypothesis of a protective role of the heterochromatin compartment adjacent to the nuclear envelope by shielding the gene-rich central region. There is yet no clear-cut explanation to heterochromatin low sensitivity to γH2AX foci formation, although the following factors have been

Table 3.1 Molecular size of selected gene-rich (HSA11, HSA19), gene-poor (HSA4, HSA18), and low gene density (HSA2) human chromosomes (Mbp) with their corresponding number of genes and radiation-induced DNA double-strand breaks (DSB) per Mbp estimated via γH2AX foci

Chromosome number	Mbp	Genes per Mbp	DSB per Mbp[a]	Number of TDRG[b]	TDRG per Mbp
2	243.6	6.2	0.05	68	0.28
4	191.7	4.8	0.03	37	0.19
11	134.4	13.75	0.07	52	0.39
18	76.1	4.3	0.03	12	0.16
19	63.8	23.9	0.12	60	0.94

Respective amounts of tumor-deregulated genes (TDRG) per chromosome and per Mbp are also depicted
[a]Data from Falk et al. (2008)
[b]Data from Folle et al. (2010)

postulated: (a) low level of histone H2AX; (b) nominal H2AX phosphorylation; (c) scarce induction of DSB because of high chromatin compaction; (d) rapid migration of genuine heterochromatic DSB to neighboring euchromatic domains; and (e) loss of heterochromatin features as a result of DSB-induced local chromatin decondensation (Cowell et al. 2007). Experimental evidence highlights the impact of chromatin relocation after DNA damage. H2AX is effectively phosphorylated in chromocenters after single-ion microbeam irradiation, but the damaged region is rapidly decondensed and shortly expelled to the chromocenter periphery (Jakob et al. 2011).

Cytogenetic evidence on the role played by chromatin structure in the localization of chromosome breakpoints induced by DNA-damaging agents (Folle 2008) has been confirmed through immunoFISH studies in nuclei of human fibroblasts (Falk et al. 2008). Results obtained indicate that genetically inactive condensed chromatin is less susceptible to DSB induction by γ-rays than are transcriptionally active regions. The amount of γH2AX foci produced by ionizing radiation in the CTs of gene-dense (HSA11, HSA19), intermediate density (HSA2), and gene-poor (HSA4, HSA18) human chromosomes was assessed. Gene-dense CTs exhibited higher yields of DNA DSB (visualized as γH2AX foci) per Mbp than intermediate or gene-poor CTs (Table 3.1).

Interestingly, damage-prone HSA11 and HSA19 harbor more tumor-deregulated genes (TDRG) per Mbp than gene-poor HSA4 and HSA18 whereas HSA 2 exhibits an intermediate yield (Folle et al. 2010) (Table 3.1). In other words, the chromosomal extent of TDRG is in agreement with damage sensitivity to ionizing radiation (see following).

The nonrandom organization of CTs within eukaryotic nuclei could influence the pattern of chromosome aberration production. Hence, nonrandom occurrence of chromosome rearrangements is expected to occur because vicinity effects and constrained migration of chromatin loops may limit the range of putative partner domains.

A good example in this respect is given by chicken DT40 (lymphocytes) and CEF (embryonic fibroblasts) cell lines. DT40 cells typically exhibit chicken gene-rich minichromosomes (MICs) in the nuclear interior whereas gene-poor macrochromosomes (MACs) dwell at the periphery (Habermann et al. 2001). Irradiated DT40 cells exhibited mainly MIC/MIC and MAC/MAC translocations. The topological partition of MICs and MACs in chicken nuclei is lost in CEF cells (MICs distribute throughout the nuclear volume), favoring neighborhoods between both chromosome types. As expected, CEF cells showed an increased frequency of MIC/MAC translocations (Grandy et al. 2002).

As mentioned earlier, CT organization and neighborhoods may differ between cell lineages, and thus variations in chromosome translocation frequencies are also expected to happen. In mouse lymphomas CT 12 and 15 are close neighbors whereas in mouse hepatomas CT 5 and 6 are topologically related. Analysis of translocation rates revealed that 5/6 rearrangements frequently occur in hepatomas but are absent in lymphomas. Conversely, 12/15 translocations prevail in lymphomas. In conclusion, the differential spatial organization of genomes in specific tissues could be critical for the formation of recurrent CA (Parada et al. 2004).

According to vicinity effects and DSB-constrained mobility, a higher frequency of chromosome rearrangements within CTs is expected to occur. However, most data point to a ratio of inter/intrachromosomal CA (F ratio) above 1; that is, an excess of interchromosome exchanges is regularly detected even for high linear energy transfer (LET) radiation where DSB are formed in close proximity along the tracks. These findings have been confirmed using high-resolution mBAND FISH and densely ionizing radiation (Johannes et al. 2004; Obe and Durante 2010). The basis of this unpredicted distribution of CA remains to be elucidated.

Recurrent translocations in Burkitt's lymphoma involve the *MYC* locus at 8q24 with different partners encoding immunoglobulin heavy chain (*IGH*, 14q21), light chain α (*IGL*, 22q11) and light chain κ (*IGK*, 2p11) gene loci. Translocation frequencies differ, being *MYC-IGH*> *MYC-IGL*> *MYC-IGK*. FISH detection of *MYC* and immunoglobulin loci with specific probes in karyotypically normal MC/CAR cells revealed a direct relationship between translocation frequencies and nuclear spatial proximity to the *MYC* locus (Roix et al. 2003). *MYC* deregulation results in nuclear remodeling of telomere and chromosome positions, preceding the onset of chromosomal rearrangements and instability (Louis et al. 2005). Spatial vicinity has been claimed as a decisive factor for some cancer-prone loci rearrangements (Gué et al. 2006; Weckerle et al. 2011) as well as for the coregulation of genes (Brown et al. 2006).

The impact of chromosome translocations on gene expression and CT repositioning has been well documented by Harewood et al. (2010). Transcriptomes pertaining to balanced translocation t(11;22)(q23;q11) carriers, Emanuel syndrome patients with +der(22)t(11;22)(q23;q11) unbalanced karyotypes, as well as from normal individuals were analyzed. Significant variations in the number of differentially expressed transcripts (DET) between translocation-carrying and normal cohorts were observed. Because Emanuel syndrome patients are partially trisomic for chromosomes 11 and 22, the expected increase in DET mapping to these regions was confirmed. In the case of balanced t(11;22)(q23:q11), many DET corresponded to genes located along the derived chromosome 11. The modification of gene expression in translocation carriers involved not only the breakpoint region but also genes residing tens of megabases apart or mapping to the opposite arm or other chromosomes. FISH studies revealed a spatial reorganization of derived chromosome 11 toward the nuclear center compared to its normal counterpart. However, no significant changes in the position of derived 22 were observed. Anchoring of NOR regions to the nucleolus could explain the constrained mobility of derived 22. It is noteworthy that a displacement of gene-rich HSA17 to a more peripheral nuclear environment was observed in translocation carriers, reflecting long-range CT modifications as a consequence of derived 11 repositioning. The authors conclude that karyotype changes may lead to large-scale variations in gene expression and alterations in CT positioning, which could impinge on genome instability, tumor development, and speciation.

Tissue-specific CT organization may drastically change in malignant cells. Variations in the location of gene-poor HSA18 and gene-rich HSA19 was observed in malignant cell lines characterized by nuclei showing inverted positional patterns and a decline in gene density nuclear order. Interestingly, positional changes of HSA18 and HSA19 have also been reported in colon carcinoma cell lines RKO and DLD1, which exhibit nearly diploid karyotypes (Cremer et al. 2003).

Chromatin Dynamics: Gene Expression and Genetic Damage

Transcriptionally competent and actively transcribed chromatin maps to the nuclear interior and roughly corresponds to domains of early-replicating, gene-rich G-light bands. Similarly, hyperacetylated histone H4 ($H4^{+a}$), a cytogenetic marker for gene expression, is also confined to the inner compartment of mammalian nuclei. These facts reveal a higher-order spatial organization of functional nuclear processes (Jeppesen and Turner 1993; Sadoni et al. 1999).

The analysis of the human transcriptome map (HTM) disclosed the presence of regions of increased gene expression (RIDGEs) as well as genome domains of very low or null transcription (antiRIDGEs). RIDGEs typically are 5- to 15-Mbp gene-dense regions exhibiting high G-C content, short introns, and SINE repeats. AntiRIDGEs, in contrast, are gene-poor, low G-C content regions that harbor longer introns and LINE repeats. Moreover, RIDGEs show open chromatin conformation (Gilbert et al. 2004) and map to the nuclear interior whereas antiRIDGEs are condensed regions adjacent to the nuclear envelope (Caron et al. 2001; Gierman and Indemans 2007).

In an attempt to disclose the putative relationship between active chromatin ($H4^{+a}$, RIDGEs) susceptibility to DNA damage induction and tumor gene deregulation, we mapped, onto human G-band idiograms: (1) radiation breakpoint clusters (RBPC; $n=69$) (Barrios et al. 1989); (2) $H4^{+a}$ regions (Jeppesen 1997); (3) the transcriptome map (Caron et al. 2001); (4) RIDGEs and antiRIDGEs (Gierman and

Indemans 2007) and; (5) tumor-deregulated genes (TDRG; $n = 1019$) (Aouacheria et al. 2006) (Fig. 3.1a, b).

TDRG cluster at 23 chromosome regions characterized by the presence of RIDGEs, $H4^{+a}$ chromatin, and RBPC. Additionally, TDRG map to 12 regions harboring RIDGEs and enriched in $H4^{+a}$ but devoid of RBPC (see 14qcen, 16p, 17q, and Xqter). Note that some chromosome segments flanking RIDGEs also concentrate TDRG (e.g., 1p, 6p, 12p, and 19q; not shown). Conversely, fewer RBPC and TDRG mapped to antiRIDGEs. RBPC exhibiting no colocalization with RIDGEs or antiRIDGEs mostly corresponded to chromosome regions of medium to high gene expression (Folle et al. 2010).

However, because there is a good correlation between the HTM and gene density maps along human chromosomes, the observed clustering of TDRG in RIDGEs could respond, at least in part, to gene content variations between gene-rich and gene-poor genome regions. Through in silico methods it was possible to determine specific chromosome subbands implicated in TDRG independent of gene concentration (Aouacheria et al. 2006). As can be seen in Table 3.2, two thirds of these subbands map to RIDGEs, harbor RBPC, and participate in amplification/deletion events in tumor formation (antiRIDGEs = 0). Nearly all subbands (32 of 33) are embedded in $H4^{+a}$ chromatin and are sites of chromosome changes during evolution.

The higher sensitivity of RIDGEs compared to antiRIDGEs in relationship to genetic damage was also observed by Falk et al. (2008). In this study, the presence of radiation-induced γH2AX foci was determined in a RIDGE (11 Mbp) as well as in a nearby antiRIDGE (11 Mbp), both mapping to the pericentric region of 11q and only 12 Mbp apart. Similar to our findings, γH2AX foci were much more frequent (~4×) in the 11q RIDGE than in the antiRIDGE in which chromatin is nearly 40 % more condensed (Goetze et al. 2007).

The concentration of RBPC and TDRG in RIDGEs and $H4^{+a}$ chromatin could be the result of a compartment-biased response to DNA insult in highly expressed regions of the human genome. In this respect, spatial CT positioning (and repositioning), neighborhoods, and intermingling of specific DNA sequences as well as long-range interactions and coexpression of genes at transcription hubs could all play a role in the origin and location of recurrent chromosomal aberrations, gene deregulation, tumor development, and karyotype evolution.

Chromatin Dynamics: DNA Replication and Genetic Damage

In mammals, replication dynamics reflects the compartmentalized structure of interphase nuclei. Replication foci (RF) can be disclosed through the incorporation of halogenated nucleotides or 5-ethynyl-2′-deoxyuridine (EdU) to S-phase cells. The progression from early to mid- and finally late DNA synthesis along the different nuclear compartments has been subdivided into five main stages: (1) RF map to the nuclear interior; (2) the pattern of RF flows to the nuclear periphery although few

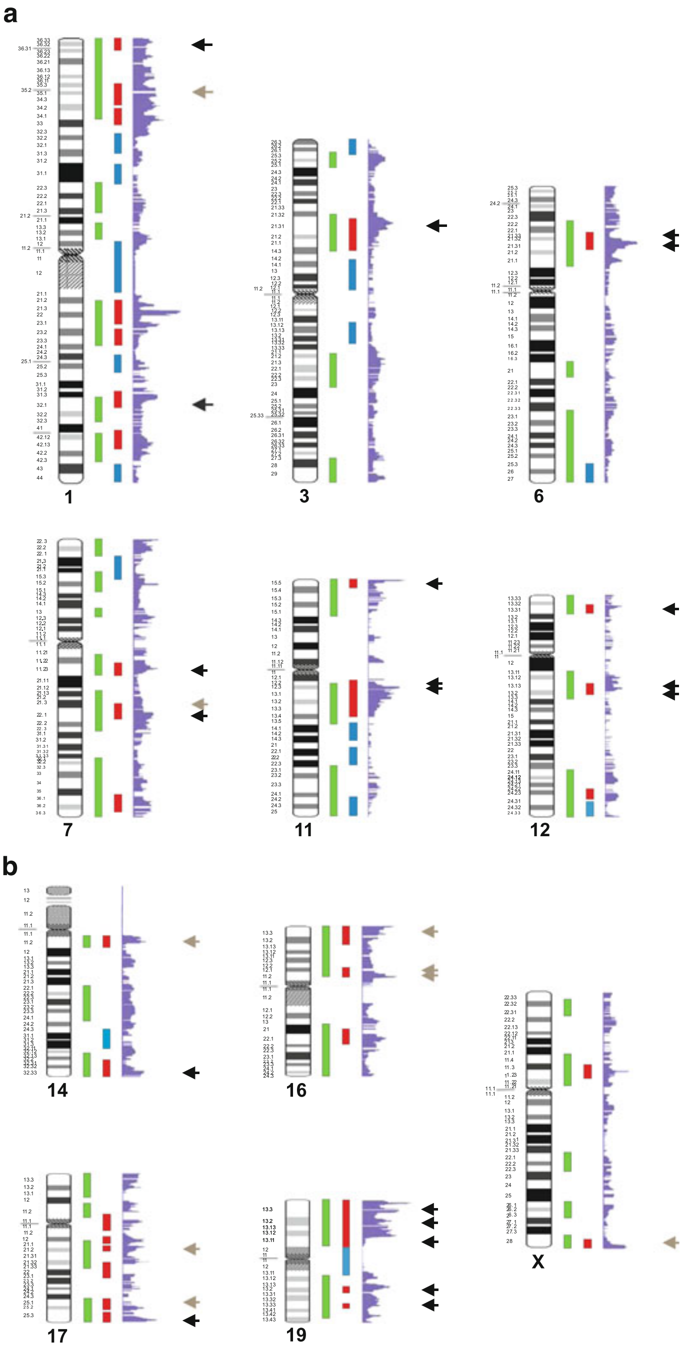

Fig. 3.1 Human idiograms depict chromosome regions harboring enriched hyperacetylated histone H4 (H4^{+a}, *green bars*), regions of increased gene expression (RIDGEs) (*red bars*), or anti-RIDGEs (*blue bars*), and the corresponding transcriptome map (*light violet*). (**a**) Chromosomes 1, 3, 6, 7, 11, and 12. (**b**) Chromosomes 14, 16, 17, 19, and X. *Black arrows* indicate colocalization of H4^{+a} chromatin with RIDGEs, clusters of radiation breakpoints (Barrios et al. 1989), and clusters of tumor-deregulated genes (TDRG) (Aouacheria et al. 2006). *Gray arrows* denote colocalization of only H4^{+a}, RIDGEs, and TDRG. (Modified from Folle et al. 2010)

Table 3.2 Colocalization of clusters of tumor-deregulated genes (TDRGs) with regions of increased gene expression (RIDGEs), antiRIDGEs, H4^{+a} chromatin, radiation breakpoint clusters (RBPC), amplification/deletion events in tumorigenesis (AMP/DEL), and breakpoints involved in evolution (EBP)

Chromosome (number of subbands)	RIDGEs	AntiRIDGEs	H4^{+a}	RBPC	AMP/DEL	EBP
1 (2)	2	0	2	2	2	2
2 (3)	0	0	3	2	0	3
3 (1)	1	0	1	1	1	1
4 (1)	0	0	1	1	0	1
5 (1)	0	0	1	0	1	1
6 (1)	1	0	1	1	1	1
7 (3)	3	0	3	2	3	3
9 (2)	1	0	2	2	2	2
11(4)	2	0	4	4	3	4
12 (2)	1	0	2	2	1	2
14 (2)	2	0	2	1	2	2
16 (2)	1	0	1	0	2	2
17 (1)	1	0	1	0	1	1
19 (5)	5	0	5	4	4	5
20 (1)	0	0	1	1	0	1
21(1)	1	0	1	0	1	1
X (1)	1	0	1	0	1	0
17 (33)	*22*	*0*	*32*	*23*	*25*	*32*

A total of 33 chromosome subbands (in 17 chromosomes) that are implicated in tumor gene deregulation independently of gene density (Aouacheria et al. 2006) are listed (see text)

inner RF persist; (3) RF map only to the nuclear border and perinucleolar regions; (4) large and fewer RF are found at the nuclear rim and central region; (5) in late S-phase cells, large RF predominate in chromocenters residing in the nuclear interior and smaller RF map to peripheral heterochromatin domains (O'Keefe et al. 1992; Sadoni et al. 1999, 2004).

Replicating chromatin has been reported to be more sensitive to DNA-damaging agents (Cowell et al. 2007). Remodeling complexes associated to DNA synthesis could enhance chromatin accessibility and favor the induction of DNA damage in chromosome regions undergoing replication (Di Tomaso et al. 2010).

An interesting model to test the role played by DNA replication and chromatin remodeling in the production of chromosome breakpoints in mammalian cells has been developed by our group (Di Tomaso et al. 2006). The model takes advantage of the peculiar chromatin organization of the X chromosome in CHO cells. The short arm (Xp) is entirely euchromatic whereas heterochromatin is confined to the long arm (Xq) with the exception of a medial conspicuous secondary constriction (Xq_{sc}). Xp (as well as Xq_{sc}) exhibit hyperacetylated chromatin whereas Xq is underacetylated (Martínez-López et al. 2001). Pulse-labeling of CHO cultures with the base analogue bromodeoxyuridine (BrdU) allowed us to precisely define in metaphase spreads the S-phase stage (early, mid, or late) in which DNA insult occurred by BrdU immunodetection with fluorochrome-tagged specific antibodies. As one would expect, BrdU labeling is restricted to Xp during early S-phase and to Xq in late S-phase, whereas a combination of both patterns is observed in cells labeled during mid S-phase. By mapping chromosome breakpoints along CHO Xp and Xq in cells damaged and labeled during early (ES) or late (LS) S-phase, it is possible to assess the influence of replication timing and remodeling processes in BP localization.

Topoisomerase II (Topo II) modulates supercoiling and alleviates torsional stress in DNA through the generation of short-lived DSB that abrogate knots and tangles (Podhorecka et al. 2010). Topo II inhibitors (i.e., etoposide) are among the most effective anticancer drugs and potent inducers of DSB by stabilizing the cleavable complex of Topo II with DNA (Palitti 1993). Rolling DNA replication forks may collide with drug-stabilized Topo II–DNA complexes, turning transient DSB produced by Topo II into permanent DSB, leading to the induction of chromosomal aberrations.

Analysis of CA induced by etoposide in ES cells showed a concentration of BP in Xp. Conversely, clustering of BP in Xq was observed in cells exposed during LS (Fig. 3.2). A similar partition in the distribution of BP in Xp and Xq according to replication time was observed when the alkylating agent methyl methanesulfonate (MMS) was assayed (Di Tomaso et al. 2006). Exposure of CHO cells to UV radiation also showed BP clustering in Xp and Xq during ES and LS, respectively (Di Tomaso et al. 2010).

However, BP clustered in Xp but not in Xq after electroporation of the restriction endonuclease *Alu*I (5′-AGCT-3′) into ES and LS CHO cells, respectively (Di Tomaso et al. 2010). In this case, it can be argued that accessibility for bulky molecules such as *Alu*I (38 kDa) could still be hampered in replicating Xq heterochromatin during late S-phase. Supporting this view is the fact that Xq is highly resistant to *Alu*I digestion in metaphase spreads of CHO cells (Folle et al. 1997).

As mentioned, synchronized MCF7 cell cultures treated with hydroxyurea showed a preferential localization of γH2AX foci in heterochromatin during LS as evidenced by colocalization with HP1. Similar findings were reported when MCF7 cells were X-irradiated or exposed to the anticancer compound cisplatin (Cowell et al. 2007). Interestingly, an increment of γH2AX foci number was also observed in γ-irradiated human BJ skin fibroblast nuclei pretreated with hypotonic culture medium (~140 mOsm) to induce chromatin decondensation (Falk et al. 2008).

The drift of DNA replication along the different nuclear compartments allows studying the spatiotemporal relationship between RF (EdU labeling) and induced DSB (γH2AX foci immunodetection) in interphase nuclei.

The localization of RF and DSB (γH2AX foci) in CHO cells induced by the radiomimetic agent bleomycin in different stages of the S-phase is shown in Fig. 3.3. Some γH2AX foci colocalize with RF while others map to the boundaries of replication compartments. Most γH2AX foci do not map to EdU-unlabeled nuclear regions in either early/mid or late S-phase. These results underscore the impact of DNA synthesis and chromatin decondensation regarding the topology of DNA damage induction.

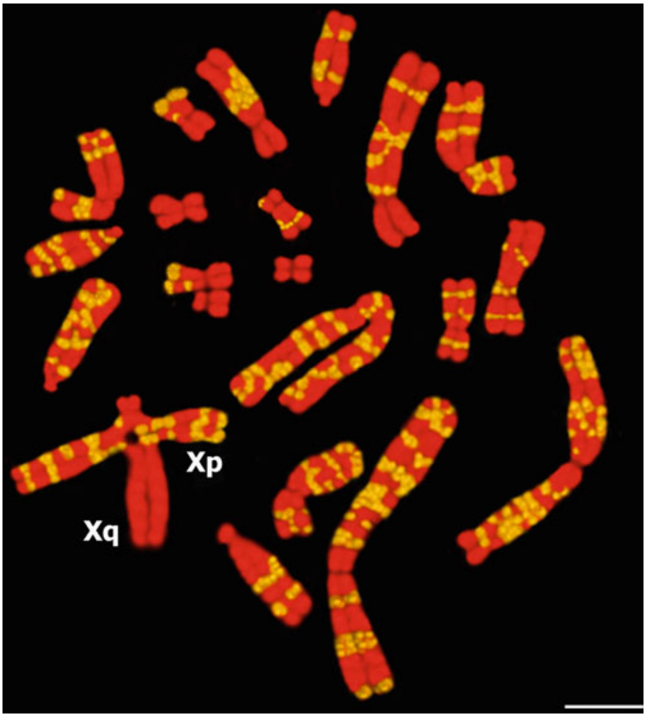

Fig. 3.2 CHO9 metaphase depicting early-replicating chromosome regions by immunodetection of BrdU incorporation using FITC-tagged anti-BrdU antibodies (*yellow*). Chromosomes were counterstained with propidium iodide (*red*). A quadrirradial rearrangement involving Xp and an acrocentric autosome is illustrated. Note the absence of replication labeling in Xq. *Bar* 5 μm

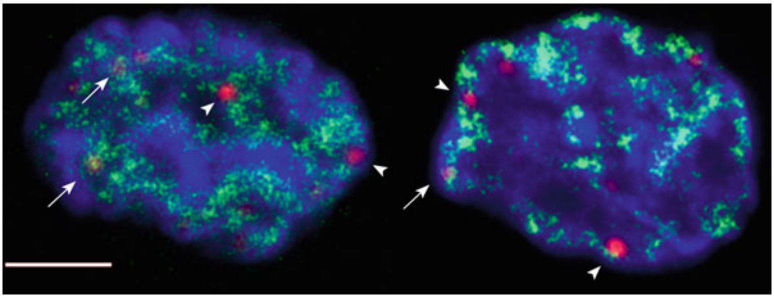

Fig. 3.3 Confocal z-sections showing the distribution of primary DNA damage (double-strand breaks, DSB) induced by bleomycin in CHO9 nuclei revealed as γH2AX foci with Cy3-bound specific antibodies (*red*) in relationship to replication foci (RF) detected with the EdU-Click-iT Alexa Fluor 488 Kit (*green*). An early/mid S-phase nucleus (*left*) and a late-replicating nucleus (*right*) are depicted. Nuclei were counterstained with DAPI. γH2AX foci positioning follows replication labeling. Colocalization of γH2AX foci with RF clusters is observed (*arrows*). γH2AX foci also map to the borders of replicating chromatin domains (*arrowheads*). (From Liddle P, unpublished results). *Bar* 3 μm

Recent findings involving the origin of somatic copy number alterations (SCNA) have shed new light concerning the participation of DNA replication in the mutational landscape of human cancer genomes. SCNA are abnormal structural variations of the genome arising through deletions or amplifications of chromosome segments. The study by De and Michor (2011) integrated databases from more than 330,000 SCNA boundaries inferred from microarray analysis of 2,792 samples pertaining to 26 different types of cancer, genome-wide DNA replication timing, and long-range (Hi-C) DNA interactions. They were able to demonstrate that SCNA arise preferentially in neighboring genomic regions (enriched for interactions in the Hi-C database) that share similar replication timing. Remarkably, early replicating regions exhibited more amplification SCNA events whereas deletions were more frequent in late-replicating domains. Thus, the spatiotemporal dynamics of DNA replication seems to play a crucial role in the generation of cancer-prone genomic rearrangements.

Conclusions

Nuclear structure and dynamics seem to impinge in the genesis and localization of CA. Genome regions with open chromatin conformation, high gene expression, or undergoing DNA replication constitute preferential sites for the induction of CA, thus paving the way for tumorigenesis. Spatial proximity may also be critical to determine partnerships in spontaneous or induced chromosome rearrangements. Correlative metaphase/interphase molecular cytogenetics has still much to offer to shed new light in the fields of chromatin organization and function, DNA damage handling, and CA production. New technological achievements that allow us to scrutinize the nuclear structure at the nanometer scale will certainly afford a new perspective to our present knowledge on the mechanisms of the origin of CA.

Acknowledgments We are indebted to PEDECIBA Postgraduate Program, the Agencia Nacional de Investigación e Innovación (ANII), and the Alexander von Humboldt-Foundation (AvH). P.L. is a former Fellow of an AvH Linkage Program research project.

References

Aouacheria A, Navratil V et al (2006) Bioinformatic screening of human ESTs for differentially expressed genes in normal and tumor tissues. BMC Genomics 7:94. doi:10.1186/1471-2164-7-94

Barrios L, Miró R et al (1989) Cytogenetic effects of radiotherapy breakpoint distribution in induced chromosome aberrations. Cancer Genet Cytogenet 41:61–70

Branco MR, Pombo A (2006) Intermingling of chromosome territories in interphase suggests a role in translocation and transcription-dependent associations. PLoS Biol 4:780–788

Brown JM, Leach J et al (2006) Coregulated human globin genes are frequently in spatial proximity when active. J Cell Biol 172(2):177–187

Caron H, van Schaik B et al (2001) The human transcriptome map: clustering of highly expressed genes in chromosomal domains. Science 291:1289–1292

Cornforth MN, Greulich-Bode M et al (2002) Chromosomes are predominantly located randomly with respect to each other in interphase human cells. J Cell Biol 159:237–244

Costes SV, Chiolo I et al (2010) Spatiotemporal characterization of ionizing radiation induced DNA damage foci and their relation to chromatin organization. Mutat Res 704:78–87

Cowell IG, Sunter NJ et al (2007) γH2AX form preferentially in euchromatin after ionising-radiation. PLoS One 2:e1057

Cremer M, Küpper K et al (2003) Inheritance of gene density-related higher order chromatin arrangements in normal and tumor cell nuclei. J Cell Biol 5:809–820

De S, Michor F (2011) DNA replication timing and long-range DNA interactions predict mutational landscapes of cancer genome. Nat Biotechnol 29(12):1103–1108. doi:10.1038/nbt.2030

Di Tomaso MV, Martínez-López W, Folle GA, Palitti F (2006) Modulation of chromosome damage localisation by replication timing. Int J Radiat Biol 82:877–886

Di Tomaso MV, Martínez-López W, Palitti F (2010) Asynchronously replicating eu/heterochromatic regions shape chromosome damage. Cytogenet Genome Res 128(1–3):111–117

Falk M, Lukášová E, Kozubek S (2008) Chromatin structure influences the sensitivity to γ-radiation. Biochim Biophys Acta 1783:2398–2414. doi:10.1016/j.bbamcr.2008.07.010

Folle GA (2008) Nuclear architecture, chromosome domains and genetic damage. Mutat Res 658:172–183. doi:10.1016/j.mrrev.2007.08.005

Folle GA, Obe G (1995) Localization of chromosome breakpoints induced by *Alu*I and *Bam*HI in Chinese hamster ovary (CHO) cells treated in G_1 phase of the cell cycle. Int J Radiat Biol 68:437–445

Folle GA, Obe G (1996) Intrachromosomal localization of breakpoints induced by the restriction endonucleases *Alu*I and *Bam*HI in Chinese hamster ovary cells treated in S-phase of the cell cycle. Int J Radiat Biol 69:447–457

Folle GA, Boccardo E, Obe G (1997) Localization of chromosome breakpoints induced by DNase I in Chinese hamster ovary (CHO) cells. Chromosoma (Berl) 106:391–399

Folle GA, Martínez-López W, Boccardo E, Obe G (1998) Localization of chromosome breakpoints: implication of the chromatin structure and nuclear architecture. Mutat Res 404:17–26

Folle GA, Liddle P, Lafon-Hughes L, Di Tomaso MV (2010) Close encounters: RIDGEs, hyperacetylated chromatin, radiation breakpoints and genes differentially expressed in tumours cluster at specific human chromosome regions. Cytogenet Genome Res 128(1–3):17–27

Gazave E, Gautier P, Gilchrist S, Bickmore WA (2005) Does radial nuclear organization influence DNA damage? Chromosome Res 13:377–388

Gierman HJ, Indemans MHJ (2007) Domain-wide regulation of gene expression in the human genome. Genome Res 17:1286–1295

Gilbert N, Boyle S et al (2004) Gene-rich domains are enriched in open chromatin fibers. Cell 118:555–566

Goetze S, Mateos-Langerak J et al (2007) The three-dimensional structure of human interphase chromosomes is related to the transcriptome map. Mol Cell Biol 27:4475–4487

Grandy I, Hardt T, Schmid M, Haaf T (2002) Effects of high-order nuclear structure and Rad51 overexpression on radiation-induced chromosome rearrangements. Cytogenet Genome Res 98:265–269. doi:10.1159/00007 1046

Grigorova M, Brand R, Xiao Y, Natarajan AT (1998) Frequencies and types of exchange aberrations induced by X-rays and neutrons in Chinese hamster splenocytes detected by FISH using chromosome-specific libraries. Int J Radiat Biol 74:297–314

Gué M, Sun J-S, Boudier T (2006) Simultaneous localization of MLL, AF4 and ENL genes in interphase nuclei by 3D-FISH: MLL translocation revisited. BMC Cancer 6:20–24. doi:10.1186/1471-2407-6-20

Habermann FA, Cremer M et al (2001) Arrangements of macro- and mini-chromosomes in chicken cells. Chromosome Res 9:569–584

Harewood L, Schütz F, Boyle S (2010) The effect of translocation-induced nuclear re-organization on gene expression. Genome Res 20(5):554–564. doi:10.1101/gr. 103622. 109

Holmquist GP (1992) Review article: chromosome bands, their chromatin flavors, and their functional features. Am J Hum Genet 51:17–37
Jakob B, Splinter J, Durante M, Taucher-Scholz G (2009) Live cell microscopy analysis of radiation-induced DNA double-strand break motion. Proc Natl Acad Sci USA 106:3172–3177
Jakob B, Splinter J et al (2011) DNA double-strand breaks in heterochromatin elicit fast repair protein recruitment, histone H2AX phosphorylation and relocation to euchromatin. Nucleic Acids Res 39(15):6489–6499. doi:10.1093/nar/gkr230
Jeppesen P (1997) Histone acetylation: a possible mechanism for the inheritance of cell memory at mitosis. Bioessays 19(1):67–74
Jeppesen P, Turner BM (1993) The inactive X chromosome in female mammals is distinguished by a lack of histone H4 acetylation, a cytogenetic marker for gene expression. Cell 74:281–289
Johannes C, Horstmann M et al (2004) Chromosome intrachanges and interchanges detected by multicolour banding in lymphocytes: searching for clastogen signatures in the human genome. Radiat Res 161:540–548
Karagiannis TC, Kn H, El-Osta A (2007) Disparity of histone deacetylase inhibition on repair of radiation-induced DNA damage on euchromatin and constitutive heterochromatin compartments. Oncogene 26:3963–3971
Korenberg JR, Rykowski MC (1988) Human genome organization: Alu, Lines and the molecular structure of metaphase chromosome bands. Cell 53:391–400
Küpper K, Köbl A et al (2007) Radial chromatin positioning is shaped by local gene density, not by gene expression. Chromosoma (Berl) 116:285–306
Louis SF, Vermolen BJ et al (2005) c-Myc induces chromosomal rearrangements through telomere and chromosome remodeling in the interphase nucleus. Proc Natl Acad Sci USA 102:9613–9618
Martínez-López W, Porro V et al (2000) Interchromosomal distribution of gamma ray-induced chromatid aberrations in Chinese hamster ovary cells. Genet Mol Biol 23:1071–1076
Martínez-López W, Folle GA, Jeppesen P, Obe G (2001) Chromosome regions enriched in hyperacetylated histone H4 are preferred sites for endonuclease- and radiation-induced breakpoints. Chromosome Res 9:69–75
Miller OJ, Therman E (2001) Human chromosomes. Springer, New York
Obe G, Durante M (2010) DNA double strand breaks and chromosomal aberrations. Cytogenet Genome Res 128:8–16
Obe G, Pffeifer P et al (2002) Chromosome aberrations: formation, identification and distribution. Mutat Res 504:17–36
O'Keefe RT, Henderson SC, Spector DL (1992) Dynamic organization of DNA replication in mammalian cell nuclei: spatially and temporally defined replication of chromosome-specific alpha satellite DNA sequences. J Cell Biol 116:1095–1110
Palitti F (1993) Mechanisms of induction of chromosomal aberrations by inhibitors of DNA topoisomerases. Environ Mol Mutagen 22(4):275–277
Parada LA, McQueen PG, Misteli T (2004) Tissue-specific spatial organization of genomes. Genome Biol 5:R44
Podhorecka M, Skladanoski K, Bozko P (2010) H2AX phosphorylation: its role in DNA damage response and cancer therapy. J Nucleic Acids 6:673–681. doi:10.4061/2011/920161
Postberg J, Lipps HJ, Cremer T (2010) Evolutionary origin of the cell nucleus and its functional architecture. Essays Biochem 48:1–24
Rogakou EP, Pilch PR et al (1998) DNA double-stranded breaks induce phosphorylation of histone H2AX on serine 139. J Biol Chem 273(10):5858–5868
Roix JJ, McQueen PG et al (2003) Spatial proximity of translocation-prone loci in human lymphocytes. Nat Genet 34:287–291
Rouquette J, Genoud C et al (2009) Revealing the high-resolution three-dimensional network of chromatin and interchromatin space: a novel electron-microscopic approach to reconstructing nuclear architecture. Chromosome Res 17:801–810

Sadoni N, Langer S et al (1999) Nuclear organization of mammalian genomes: polar chromosome territories build up functionally distinct higher order compartments. J Cell Biol 146(6):1211–1226

Sadoni N, Cardoso MC et al (2004) Stable chromosomal units determine the spatial and temporal organization of DNA replication. J Cell Sci 117:5353–5365

Simpson PJ, Savage JR (1995) Estimating the true frequency of X-ray-induced complex chromosome exchanges using fluorescence in situ hybridization. Int J Radiat Biol 67:37–45

Slijepcevic P, Natarajan AT (1994) Distribution of radiation-induced G_1 exchange and terminal deletion breakpoints in Chinese hamster chromosomes as detected by G-banding. Int J Radiat Biol 66:747–755

Solovei I, Kreysing M et al (2009) Nuclear architecture of rod receptor cells adapt to vision in mammalian evolution. Cell 137:356–368

Tanabe H, Habermann FA, Solovei I, Cremer M, Cremer T (2002) Non-random radial arrangements of interphase chromosome territories: evolutionary considerations and functional implications. Mutat Res 504:37–45

Weckerle AB, Santra M et al (2011) *CBFB* and *MYHII* in inv(16)(p13q22) of acute myeloid leukaemia displaying close spatial proximity in interphase nuclei of human hematopoietic stem cells. Genes Chromosomes Cancer 50:746–755

Xiao Y, Natarajan AT (1999) Non-proportional involvement of Chinese hamster chromosomes 3, 4, 8 and 9 in X-ray-induced chromosomal aberrations. Int J Radiat Biol 75:943–951